

## New Concepts

---

### Kinetic Study of DNA Condensation by Cationic Peptides Used in Nonviral Gene Therapy: Analogy of DNA Condensation to Protein Folding<sup>†</sup>

Miriam Tecle, Monika Preuss,\* and Andrew D. Miller\*

*Imperial College Genetic Therapies Centre, Flowers Building, Department of Chemistry, Armstrong Road, Imperial College London, London SW7 2AZ, United Kingdom*

*Received February 26, 2003; Revised Manuscript Received June 24, 2003*

**ABSTRACT:** Synthetic nonviral vector systems are attractive because of their apparent simplicity of preparation and use. However, there are many barriers to success at the moment, including the formulation of uniform and reproducible particles of transfection competent, condensed nucleic acids such as plasmid DNA (pDNA). For this reason, we have been studying the kinetics of cationic peptide-mediated pDNA condensation and the reverse process following peptide dissociation by stopped-flow techniques under conditions commonly used to prepare synthetic nonviral vector systems. We observe that the process of pDNA condensation and the reverse process of pDNA expansion appear to be equivalent to protein folding and unfolding, respectively. We also observe chaotic behavior at low peptide/pDNA ratios that becomes more uniform at higher ratios suggesting that with suboptimal ratios, pDNA is condensing in a multitude of conformations, each representing different stages of hydrophobic collapse in the search for the thermodynamically most stable (i.e., the fully condensed pDNA molecule). At higher ratios, peptide/pDNA complexes formed appear to be increasingly irreversible consistent with the formation of kinetically and/or thermodynamically stable, condensed pDNA molecules. Such stable states could create problems for the successful transcription of pDNA post delivery to cells.

In vivo, DNA is usually associated with cationic proteins or peptides such as protamine in sperm, histones in chromatin, and certain viral proteins in viruses that condense DNA through their cationic amino acid residues. This property of cationic peptides is commonly exploited in the context of nonviral gene therapy where precondensation of transgenic DNA is a necessary prerequisite to successful gene transfer (1–5). In our laboratory, two key cationic peptides are the 19-amino acid adenovirus core peptide  $\mu$  ( $\mu$ ,

MRRAH HRRRR ASHRR MRGG; 2440 Da) and a 23-amino acid peptide derived from the adenovirus core protein V (pepV, RPRRR ATTRR RTTGT TRRRR RRR; 3036 Da) (6–9). For our gene transfection purposes, complexes at a ratio of 0.6 peptide to plasmid DNA (pDNA) (w/w) were found to be most suitable since the resulting particles retain a slight negative charge to facilitate their interaction with cationic liposomes (6). We were able to relate the peptides' ability to precondense pDNA with a complex-stabilizing effect in biological fluids, a central criterion for successful in vivo gene therapy (6, 10, 11). However, the actual process of DNA condensation is not very well-understood, and consequently, a question mark remains over the effect of in vitro precondensation on the capacity for successful gene

<sup>†</sup> We thank the Mitsubishi Chemical Corporation for supporting the Genetic Therapies Centre at Imperial College and the work presented here.

\* To whom correspondence should be addressed. Tel.: +44 20 7594 5773. Fax: +44 20 7594 5803. E-mail: (A.D.M.) a.miller@imperial.ac.uk; (M.P.) m.preuss@imperial.ac.uk.

transcription. We recently obtained evidence suggesting that complexes of DNA and cationic peptides can readily dissociate in cells *in vitro* (8, 9) and some suggestion that some irreversible association can take place. The consequence of the latter may be impeded transcription since DNA is likely to have to dissociate from the cationic carriers to be read by the host transcriptional machinery (5, 12), whereas early dissociation would mean that DNA is condensed inadequately following cell entry to effect proper nuclear entry (8, 9). Furthermore, simple mixing of DNA and polycations usually produces particles displaying a multitude of shapes and sizes (13–18). These observations raise questions over the ability to control the formation of homogeneous particles at ratios below the point of DNA charge neutralization. We set out, therefore, to look at the process of DNA condensation in more detail, and we hereby report the findings of a study in which we attempted to characterize the process of condensation of a pDNA model (pUMVC1, 7.52 kbp; average nucleotide molecular weight 329 Da) by kinetic analysis of peptide/DNA interactions *in vitro*.

## RESULTS

**Nature of the Binding Curves.** A stopped-flow fluorimeter setup was employed (SFM-3, BioLogic) to monitor peptide/DNA complex formation and pDNA condensation using two different fluorescent probes. On one hand, the fluorescence of ethidium bromide (EtBr) upon intercalation with pDNA was monitored using an excitation wavelength of 260 nm. EtBr fluoresces strongly when bound to DNA, and the displacement of EtBr upon interaction with cationic peptides results in a decrease in fluorescence intensity that correlates with pDNA peptide binding. Figure 1 shows a representative example of a trace obtained for the interaction of  $\mu$  peptide with pDNA in the presence of EtBr. The data were best described by a nonlinear curve fit with two exponentials, yielding two observed association rate constants ( $k_{\text{obs}}$ ) and fluorescence amplitudes. Since the association/dissociation of EtBr occurred within the dead-time of mixing, these association rates are EtBr exclusion rates that monitor the rate-determining process of pDNA condensation by peptide binding. Equivalent decreases in fluorescence are also observed in ethidium bromide exclusion assays from which our stopped flow protocols here were initially derived (19, 20).

Since this approach did not follow peptide binding directly, we also used a  $\mu$  peptide analogue that was N-terminally labeled with a dansyl reporter group as a second fluorescent probe (Dn- $\mu$ ). Binding experiments with Dn- $\mu$  in the absence/presence of EtBr were performed by monitoring the fluorescence on excitation either at 260 nm (to follow the exclusion of EtBr by binding of Dn- $\mu$ ) or 323 nm (to follow the binding of Dn- $\mu$  directly). As expected, the interaction of Dn- $\mu$  with DNA resulted in an increase in dansyl fluorescence intensity. However, this binding event took place within the dead-time of mixing, and no kinetic binding curve was observed regardless of whether the data were obtained in the presence or absence of EtBr (data not shown). However, when binding of Dn- $\mu$  and DNA was reexamined by following the fluorescence of EtBr, a kinetic binding curve similar to that of Figure 1A was promptly reestablished. This result confirmed that  $k_{\text{obs}}$  values are a function of pDNA state change.

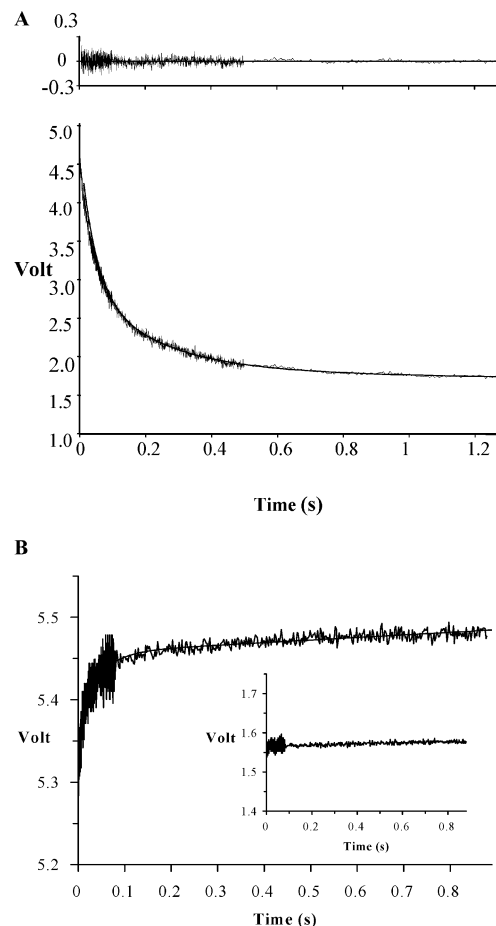


FIGURE 1: (A) Representative experimental trace showing the binding of  $\mu$  peptide to DNA (in EtBr). A total of 20  $\mu\text{L}$  of  $\mu$  peptide (24  $\mu\text{g}/\text{mL}$ ) was mixed into 30  $\mu\text{L}$  of DNA (26.6  $\mu\text{g}/\text{mL}$ ) in EtBr and made 100  $\mu\text{L}$  with 4 mM HEPES pH 7.0 ( $\mu/\text{DNA}$  ratio 0.6 w/w,  $\pm 0.7$ ). The final DNA and EtBr concentrations were 8  $\mu\text{g}/\text{mL}$  and 0.3 mg/mL respectively. The fluorescence was measured on excitation at 260 nm and collected using a cutoff filter at 345 nm. All experiments were performed in 4 mM HEPES pH 7.0 at 20 °C. The data were best described by nonlinear curve fitting with two exponentials (see top panel for goodness of fit). No curve was observed for the dissociation of EtBr and DNA in the absence of peptide, confirming that the observed event was related to peptide binding. (B) Dissociation curves obtained for Dn- $\mu$ /DNA complexes at a ratio of 1.2 w/w ( $\pm 1.4$ ) in the presence of EtBr. Main graph, excitation at 260 nm; inset, excitation at 323 nm. A total of 105  $\mu\text{L}$  of 4 mM HEPES pH 7.0 in 4  $\mu\text{g}/\text{mL}$  EtBr was mixed with 45  $\mu\text{L}$  of Dn- $\mu$ /DNA complex (26  $\mu\text{g}/\text{mL}$  DNA). The emitted light was selected using a cutoff filter of 345 nm.

Similar results were obtained when preformed complexes of  $\mu$ :DNA and Dn- $\mu$ :DNA were diluted to follow dissociation kinetics. The process could only be observed by following the increase in EtBr fluorescence intensity (Figure 1B). This confirmed that the dissociation rate constants obtained were not due to the dissociation of the peptide but related to pDNA structural rearrangements and consequential reassociation of EtBr. Dissociation kinetics traces were fitted accurately by a triple exponential function giving three rate constants for EtBr inclusion, themselves equivalent to rates of pDNA expansion and state changes.

Table 1 lists the values for the observed rate constants obtained from curve fitting of the respective experimental results. EtBr exclusion rates ( $k_{\text{obs}}$ ) for Dn- $\mu$ :DNA complexes were about twice as fast as those of  $\mu$ :DNA, a finding

Table 1: Comparison of the Observed Rates of pDNA Condensation (EtBr Exclusion,  $k_{\text{obs}}$ ) and pDNA Expansion (EtBr Inclusion,  $k_{\text{diss}}$ ) as Mediated by  $\mu$  or Dn- $\mu$  Binding to pDNA<sup>a</sup>

complex	$k_{\text{obs}} (\text{s}^{-1})$ (0.6 w/w, $\pm 0.7$ )		$k_{\text{diss}} (\text{s}^{-1})$ (1.2 w/w, $\pm 1.4$ )		
	rate 1	rate 2	rate 1	rate 2	rate 3
Dn- $\mu$ /DNA	225 $\pm$ 37	30.4 $\pm$ 5	273 $\pm$ 42	24.5 $\pm$ 6	1.7 $\pm$ 1
$\mu$ /DNA	116 $\pm$ 10	14.2 $\pm$ 3	46 $\pm$ 9	9.2 $\pm$ 3	1.0 $\pm$ 0.3

<sup>a</sup> Data were obtained in 4 mM HEPES pH 7.0 at 20 °C as described in the legend to Figure 1 and in the text. Ratios refer to the weight of peptide to DNA. For comparison, folding of two-state proteins generally occurs with folding rates between 10 and 1000  $\text{s}^{-1}$  (30).

consistent with competition between the dansyl label and EtBr for DNA binding sites. Correspondingly, the rates of EtBr inclusion ( $k_{\text{diss}}$ ) were also significantly greater for Dn- $\mu$  peptide consistent with both the release of a greater number of EtBr-DNA binding sites upon peptide release but also a faster peptide dissociation rate in line with previously published results showing that Dn- $\mu$  binds DNA more weakly than  $\mu$  peptide (9).

**Varying Peptide Concentration.** Having established the nature of the binding curves, we then performed a series of titration experiments where we added varying amounts of peptide into a fixed concentration of DNA. The resulting data were expressed in terms of their respective amplitudes and observed rate constants of EtBr exclusion (DNA condensation) as a function of the peptide concentration. The data for pepV are shown (Figure 2A), similar results were found with  $\mu$  or protamine sulfate, a third cationic peptide that is used commonly as a DNA charge-neutralizing and condensing agent in gene therapy (PRRRR SSSRP VRRRR RPRVS RRRRR RGGR RR; 4250 Da) (2, 10, 11, 21, 22). The amplitudes were found to increase in magnitude with the peptide concentration until saturation was achieved at ratio of 1.4 w/w, indicating the ratio of maximum exclusion of EtBr and extent of DNA condensation (Figure 2A, inset). The observed rate constants were found to be chaotic and irreproducible for ratios below 1.4 w/w. We would like to note that theoretical charge/molecular weight ratios of all three peptides are approximately equivalent; hence, calculated w/w ratios also turn out to be reasonable estimations of theoretical  $\pm$  ratios. Hence, w/w ratios were used throughout here and for the sake of consistency with our previous biophysical characterizations of peptide/pDNA characterizations (6, 8, 9). Furthermore, according to our previous data, peptide:pDNA complex aggregation was not observed (as observed by photon correlation spectroscopy) with either  $\mu$ :pDNA or protamine:pDNA complexes even up to a 1.4 w/w ratio when the theoretical  $\pm$  ratio is  $>1$  (6, 9). The same appears to be true of pepV:pDNA complexes (unpublished data). Hence, the concentration dependent experimental data described here should be largely free of complications from aggregation, at least initially.

**Dissociation of Peptide:DNA Complexes.** Dissociation experiments of peptide:DNA complexes were performed to obtain rate constants of EtBr inclusion following pDNA expansion ( $k_{\text{diss}}$ ). These were independent of the dilution factor so long as the ratio between the components was greater than 0.6 w/w (data not shown). However, the rate constants were affected by the actual ratio of peptide:DNA at low ratios (Figure 2B). Broadly,  $k_{\text{diss}}$  values for all peptides

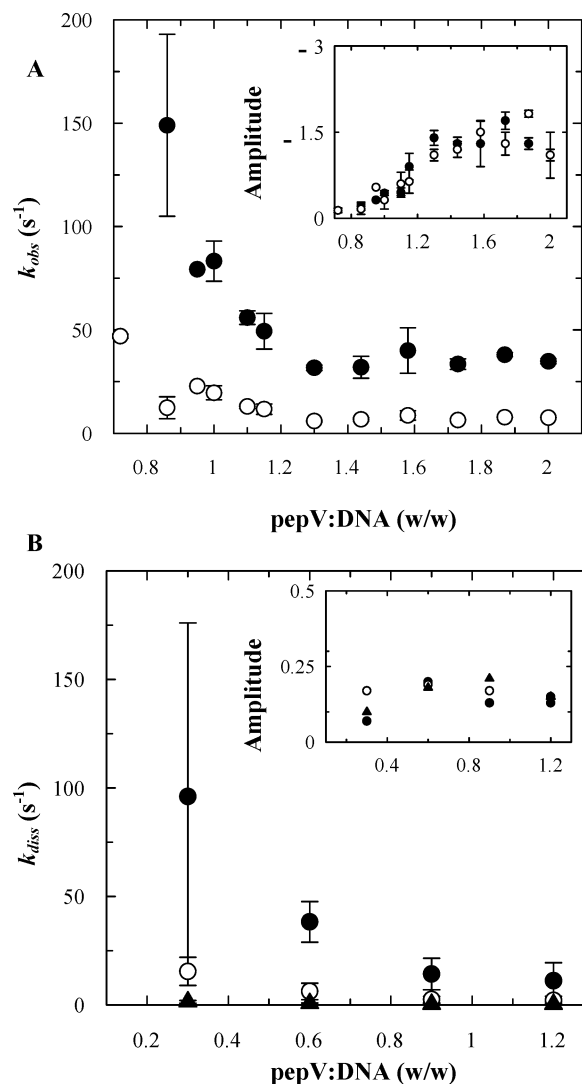


FIGURE 2: (A) Fluorescence amplitudes (inset) and rate constants of EtBr exclusion ( $k_{\text{obs}}$ ) following the interaction of pDNA with pepV. Similar results were obtained with  $\mu$  or protamine sulfate. Values were obtained from the fitting of the experimental association curves to a double exponential decay function. Values of amplitude and rate 1 (●) and amplitude and rate 2 (○) were plotted as a function of the pepV/DNA ratio. Three experiments were averaged per data point, and each data point was repeated three times. Error bars show the standard deviation. Appropriate volumes of 4 mM HEPES pH 7.0 were added to keep the final concentration of DNA constant. (B) Total fluorescence amplitude (inset) and rate constants of EtBr inclusion ( $k_{\text{diss}}$ ) following the dissociation of pepV/DNA complexes ( $k_{\text{diss}}$ ). Values of rate 1 (●), rate 2 (○), and rate 3 (▲) are plotted as a function of the pepV/DNA ratio. Error bars show the standard deviation of 10 experiments. For details, see legend to Figure 1.

were irregular at low ratios and stabilized toward higher weight ratios, thereby mirroring results from association studies (cf. Figure 2A). Furthermore, at higher weight ratios, we also found that complex dissociation was increasingly irreversible as suggested by the fall in fluorescence amplitude with increasing ratios. For example, Figure 2B (inset) shows fluorescence changes on dissociation of pepV:DNA as a function of the pepV concentration. The apparent failure of recovery of EtBr fluorescence with increasing peptide:pDNA ratios suggests that particles dissociated less efficiently and/or that pDNA expansion was less efficient as the peptide concentration was increased. This could be due to irreversibly bound peptide molecules that cross-link individual DNA



particles (12, 23, 24) and/or due to the fact that collapsed DNA molecules are thermodynamically more stable than the initial supercoiled particles.

## DISCUSSION

Association studies of fluorescent  $\mu$  peptide (Dn- $\mu$ ) and pDNA demonstrated binding to occur within milliseconds, the dead-time of mixing of our stopped flow apparatus. This necessitated the use of EtBr as an indirect monitor of binding but at the same time allowed us to observe the consequential event(s) of DNA collapse. The interaction between pDNA and peptide involves multiple binding sites, approximately 1300 for  $\mu$ , 800 for pepV, and 400 for protamine (9) (unpublished observation) the binding of which result in exclusion of EtBr, DNA charge neutralization, hydrophobic collapse, and condensation. Bearing in mind the great size difference between pDNA (7.5 kbp) and peptides, the binding of a single polypeptide to a plasmid molecule is likely to affect local DNA secondary and tertiary structure, thereby causing a perturbation that extends somewhat beyond the segment of pDNA molecule occupied by the peptide. Presumably, this influences the binding of a second polypeptide adjacent to the first (intramolecular cooperativity) and leads to eventual plasmid condensation and collapse. Cooperativity of peptide-mediated pDNA collapse appears to be substantiated by the sigmoidal shape of the plot showing the amplitudes (Figure 2A). A similar mechanism has been proposed following the interaction of other cationic peptides and proteins such as protamine, poly-lysine, and histones with DNA (12, 23, 25). Given the complexity of the system, it is difficult to attribute actual events to the experimental rate constant values. Nevertheless, since peptide binding to pDNA and EtBr binding to pDNA (in the absence of peptide) were both shown to be instantaneous processes, it can be speculated that the two observed rate constants of EtBr exclusion illustrate two phases of DNA hydrophobic collapse. Conversely, the three rate constants of EtBr inclusion may describe three phases of DNA expansion such as relaxation plus pDNA reopening and structural readjustments.

The great variation of the rate constants at suboptimal conditions but stabilization at ratios beyond full condensation (Figure 2) reminds us of the funnel energy landscape theory of protein folding (26, 27). Here, intermediate protein folding states are seen as ensembles of individual chain conformations of similar energy in a biased search for the minimum on an energy surface. The funnel view postulates that there are many ways for an unfolded, highly disordered polypeptide chain to reach the native and thermodynamically most stable form of the protein. This bias in folding arises as the many conformations of the unfolded states adopt a progressively smaller number of states, thereby reducing their lower free energy until the molecule reaches its most stable form, the native conformation of minimal free energy (28). In analogy to this folding funnel approach for proteins, we would like to put forward the idea that the peptide-mediated condensation of pDNA occurs by a similar mechanism to the hydrophobic collapse of protein folding intermediates. This is an expansion of the recognition that similarities exist between some aspects of DNA condensation and protein folding (29). We postulate that suboptimal ratios of peptide/DNA (e.g., ratios below 1.4 w/w for pepV) each represent different stages of hydrophobic collapse on an energy surface

representing kinetically and/or thermodynamically trapped intermediates. Increasing amounts of peptide reduce the number of conformations until the fully condensed, saturated, collapsed, and therefore most stable form of the molecule is reached, the global minimum. The fact that complex dissociation was progressively more incomplete (Figure 2B) corroborates the proposition that condensed DNA is thermodynamically more stable and in a state of lower free energy than the supercoiled form. By analogy to proteins, therefore, the folding and unfolding of DNA can be simulated by the addition and removal of condensing peptide, respectively. Further, two-state proteins are known commonly to fold with rates ranging from  $\sim 10$  to  $1000 \text{ s}^{-1}$  comparable with our observed DNA condensation rates (cf. Table 1) (30).

The way in which complexes between DNA and cationic peptides are prepared affects the nature of the resulting particles. For instance, size measurements using photon correlation spectroscopy revealed that rapid mixing of individual solutions of peptide and DNA at different ratios results in smaller and more defined complexes than the slow and stepwise titration of components into preformed complexes (unpublished observations), highlighting differences between kinetically and thermodynamically driven processes. Indeed, it has been known for some time that rapid mixing of DNA and cationic proteins/peptides produces complexes that are different from those produced by thermodynamic annealing through gradient dialysis (23, 24). Again, an analogy can be made with protein hydrophobic collapse where different conformations can be obtained—native and misfolded—as a function of the environment and extrinsic folding/refolding conditions (28, 31). Reversibility of complex formation is an important consideration in gene therapy with potential consequences for the transcriptional activity of precondensed pDNA. For example, in vivo protamine: DNA complexes in sperm are transcriptionally inactive owing to the ability of adjacent arginine residues to interlock both strands of the helix (12). Brewer et al. in their kinetic studies involving DNA toroid formation also noted the incomplete dissociation of protamine from DNA, an observation that is completely consistent with our data (Figure 2B). On the basis of this result, the authors argued that an active mechanism must be in place in vivo to remove protamine from sperm DNA to activate the genome after fertilization (12, 32).

In addition to providing insights into the mechanism of supercoiled pDNA condensation by charge-neutralizing peptides, this paper presents some important conclusions for nonviral gene therapy. The difficulty of controlling peptide: DNA complex formation and producing homogeneous, fully condensed particles may go some way toward offering an explanation for the recurrent irreproducibility and disappointing efficacy of many nonviral gene transfer experiments. On the basis of the results presented here, we come to the conclusion that the heterogeneity of complexes is an intrinsic feature of any such formulation systems. Perhaps, one way forward could be to concatenate several cationic peptide molecules ( $\mu$  and/or pepV), thereby creating a polymer-like molecule with several functions (DNA condensation and/or NLS). Such a molecular scaffold potentially could facilitate the condensation of pDNA in a more controlled manner than the current method of condensation via a multitude of individual and ill-defined binding events. Attempts to

synthesize such a molecule are currently under way in our laboratory.

## REFERENCES

1. Wagner, E., Cotten, M., Foisner, R., and Birnstiel, M. L. (1991) *Proc. Natl. Acad. Sci. U.S.A.* 88, 4255–9.
2. Gao, X., and Huang, L. (1996) *Biochemistry* 35, 1027–36.
3. Machy, P., and Leserman, L. D. (1983) *Biochim. Biophys. Acta* 730, 313–20.
4. Miller, C. R., Bondurant, B., McLean, S. D., McGovern, K. A., and O'Brien, D. F. (1998) *Biochemistry* 37, 12875–83.
5. Zabner, J., Fasbender, A. J., Moninger, T., Poellinger, K. A., and Welsh, M. J. (1995) *J. Biol. Chem.* 270, 18997–9007.
6. Tagawa, T., Manvell, M., Brown, N., Keller, M., Perouzel, E., Murray, K. D., Harbottle, R. P., Tecle, M., Booy, F., Brahimi-Horn, M. C., Coutelle, C., Lemoine, N. R., Alton, E. W., and Miller, A. D. (2002) *Gene Ther.* 9, 564–76.
7. Murray, K. D., Etheridge, C. J., Shah, S. I., Matthews, D. A., Russell, W., Gurling, H. M., and Miller, A. D. (2001) *Gene Ther.* 8, 453–60.
8. Keller, M., Harbottle, R. P., Perouzel, E., Colin, M., Shah, I., Rahim, A., Vaysse, L., Bergau, A., Moritz, S., Brahimi-Horn, C., Coutelle, C., and Miller, A. D. (2003) *ChemBioChem* 4, 286–98.
9. Keller, M., Tagawa, T., Preuss, M., and Miller, A. D. (2002) *Biochemistry* 41, 652–9.
10. Sorgi, F. L., Bhattacharya, S., and Huang, L. (1997) *Gene Ther.* 4, 961–8.
11. Li, S., Rizzo, M. A., Bhattacharya, S., and Huang, L. (1998) *Gene Ther.* 5, 930–7.
12. Brewer, L. R., Corzett, M., and Balhorn, R. (1999) *Science* 286, 120–3.
13. Kwoh, D. Y., Coffin, C. C., Lollo, C. P., Jovenal, J., Banaszczuk, M. G., Mullen, P., Phillips, A., Amini, A., Fabrycki, J., Bartholomew, R. M., Brostoff, S. W., and Carlo, D. J. (1999) *Biochim. Biophys. Acta* 1444, 171–90.
14. Chesnoy, S., and Huang, L. (2000) *Annu. Rev. Biophys. Biomol. Struct.* 29, 27–47.
15. Molas, M., Bartrons, R., and Perales, J. C. (2002) *Biochim. Biophys. Acta* 1572, 37–44.
16. Aris, A., and Villaverde, A. (2000) *Biochem. Biophys. Res. Commun.* 278, 455–61.
17. Chan, C. K., Senden, T., and Jans, D. A. (2000) *Gene Ther.* 7, 1690–7.
18. Birchall, J. C., Kellaway, I. W., and Gumbleton, M. (2000) *Int. J. Pharm.* 197, 221–31.
19. Stewart, L., Manvell, M., Hillery, E., Etheridge, C. J., Cooper, R. G., Stark, H., van-Heel, M., Preuss, M., Alton, E. W. F. W., and Miller, A. D. (2001) *J. Chem. Soc., Perkin Trans. 2*, 624–32.
20. Preuss, M., Tecle, M., Shah, I., Matthews, D. A., and Miller, A. D. (2003) *Org. Biomol. Chem.* 1, 2430–8.
21. Li, S., and Huang, L. (1997) *Gene Ther.* 4, 891–900.
22. Whitmore, M., Li, S., and Huang, L. (1999) *Gene Ther.* 6, 1867–75.
23. Shapiro, J. T., Leng, M., and Felsenfeld, G. (1969) *Biochemistry* 8, 3119–32.
24. Adler, A. J., and Fasman, G. D. (1971) *J. Phys. Chem.* 75, 1516–26.
25. Fasman, G. D., Schaffhausen, B., Goldsmith, L., and Adler, A. (1970) *Biochemistry* 9, 2814–22.
26. Bryngelson, J. D., Onuchic, J. N., Socci, N. D., and Wolynes, P. G. (1995) *Proteins* 21, 167–95.
27. Dill, K. A., and Chan, H. S. (1997) *Nat. Struct. Biol.* 4, 10–9.
28. Dobson, C. M. (2001) *Philos. Trans. R. Soc. London, Ser. B* 356, 133–45.
29. Bloomfield, V. A. (1996) *Curr. Opin. Struct. Biol.* 6, 334–41.
30. Roder, H., and Colon, W. (1997) *Curr. Opin. Struct. Biol.* 7, 15–28.
31. Damaschun, G., Damaschun, H., Gast, K., and Zirwer, D. (1999) *J. Mol. Biol.* 291, 715–25.
32. Ruiz-Lara, S., Cornudella, L., and Rodriguez-Campos, A. (1996) *Eur. J. Biochem.* 240, 186–194.

BI034325E